Journal of Applied Polymer Science

Synthesis, Characterization, and UV-Curing Properties of Silicon-Containing (Meth)acrylate Monomers

Siyuan Wang, Yingquan Zou
College of Chemistry, Beijing Normal University, Haidian District, Beijing 100875, China
Correspondence to: Y. Q. Zou (E-mail: zouyq@263.net)

ABSTRACT: Eight different silicon-containing (meth)acrylate monomers are synthesized by the substitution reaction of chlorosiloxanes with 2-hydroxyethyl methacrylate or 2-hydroxyethyl acrylate. Their molecular structures are confirmed by IR, ^{1}H-NMR, and ^{13}C-NMR spectroscopic analyses. The effects of silicon content on the UV-curing behavior, physical, surface, and thermal properties are investigated. The UV-curing behavior is analyzed by photo differential scanning calorimetry. The surface free energy of the UV-cured film is calculated from contact angles measured using the Lewis acid-base three liquids method. The silicon-containing (meth)acrylate monomers perform much better than traditional (meth)acrylate monomers on UV-curing. The silicon-containing monomers have higher final conversions and fast UV-curing rates in photopolymerization. The surface free energy decreases with increasing silicon content, because silicon in the soft segment is transferred to the surface, producing a UV-cured film; this is confirmed by X-ray photoelectron spectroscopy measurements. All these advantageous properties enable these synthetic silicon-containing monomers to perform better in applications. © 2013 Wiley Periodicals, Inc. J. Appl. Polym. Sci. 129: 3325–3332, 2013

KEYWORDS: synthesis and processing; monomers; oligomers and telechelics; photopolymerization

Received 23 September 2012; accepted 9 December 2012; published online 25 February 2013
DOI: 10.1002/app.38943

INTRODUCTION

As alternatives to traditional thermally cured and solvent-based resins, UV-curable systems are widely used in various industries because of their benefits such as high efficiency, environmental friendliness, and energy saving.[1] Until now, (meth)acrylate monomers have been commonly used in photopolymerization.[2,3] Further improvements in resists aim to enhance their thermal stability, to enable them to be released from matrixes and to increase their final conversions and UV-curing rates. Modified (meth)acrylate monomers are used in a wide range of applications.[4–6] Silicon-containing monomers are promising UV-curing resists because of the outstanding bulk properties of silicon such as chemical and thermal stability, and also because they can give low adhesion, good weathering resistance, and two sites for cross-linking or functional side-groups through bond formation with silicon.[7] Moreover, the hydrophobicity, flexibility, and antifouling properties of the siloxane backbone ($[Si—O]_n$ units) make polysiloxanes excellent materials for the production of electronic devices, and the protection of optical fibers, glass, metals, wood, and plastics.[8] Polysiloxanes can also be used in nanoimprinting, water-repellent coatings,[9–11] and fingerprint-resistant materials.

Many silicon-containing monomers have already been synthesized, investigated, and applied in different fields.[12,13] A number of diacrylates and triacrylates and methacrylates containing silicon have been prepared,[14,15] but the surface free energies of monomers with only one silicon atom are not low enough to obtain good releasability and antifouling properties. However, to the best of our knowledge, there is no published work addressing the synthesis and investigation of (meth)acrylate monomers with more than one silicon atom.

In this study, (meth)acrylate monomers with one to four silicon atoms were synthesized using a dehydrochlorination condensation reaction. These eight synthetic monomers were compared with (meth)acrylate monomers without silicon atoms, in terms of their thermal and surface properties, and their UV-curing behaviors. The effects of silicon content on these properties were also investigated.

EXPERIMENTAL

Materials

2-Hydroxyethyl methacrylate (2-HEMA), 2-hydroxyethyl acrylate(2-HEA), dichlorosilane, and 1,4-butanediol diacrylate were purchased from Alfa Aesar (Tianjin, China).

Additional Supporting Information may be found in the online version of this article.

© 2013 Wiley Periodicals, Inc.

Journal of Applied Polymer Science

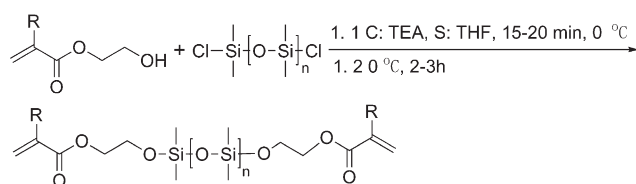

Scheme 1. Synthesis of silicon-containing (meth)acrylate monomers (R = CH_3 or H; $n = 0, 1, 2, 3$).

1,3-Dichlorotetramethyldisiloxane, 1,5-dichlorohexamethyltrisiloxane, 1,7-dichlorooctamethyltetrasiloxane, and 1,4-butanediol dimethacrylate were provided by Meryer (Shanghai, China). Tetrahydrofuran (THF), hexane, and triethylamine (TEA) were purchased from the Sinopharm Group Chemical Reagent (Beijing, China). 2-Isopropylthioxanthone (ITX) and 2-methyl-4-(methylthio)-2-morpholinopropiophenone (Irgacure 907) were provided by Shenzhen Rongda Electronic Material (Shenzhen, China). All reagents were purified according to standard laboratory methods.

Synthesis of Silicon-Containing (Meth)acrylate Monomers

Eight different silicon-containing (meth)acrylate monomers were synthesized according to the process shown in Scheme 1. A typical procedure for the reaction of 2-HEA with 1,3-dichlorotetramethydisiloxane is used as an example. 1,3-Dichlorotetramethydisiloxane (4.064 g, 0.02 mol), TEA (4.048 g, 0.04 mol), and THF (60 mL) were placed in a three-necked round-bottomed flask equipped with a mechanical stirrer and a nitrogen inlet, and cooled by an ice-bath. 2-HEA (4.644 g, 0.04 mol) dissolved in THF (40 mL) was added from a dropping funnel. The reactivity of substitution reaction of the hydroxyl group (OH) by the halogen group (Cl) is very high. The reaction occurred immediately after contact of the reagents, so the dropping speed of 2-HEMA or 2-HEA was adjusted to a sufficiently slow rate. After addition of the reagents was complete (about 15 min), the reactants were stirred for 2–3 h in the flask, which was kept in the ice-bath. The ice bath is important because the low temperature inhibits decomposition of the silicon-containing monomers in the solvent, and the substitution reaction is an exothermic reaction. The results indicated that a lower temperature could improve the yield. The product was filtered to remove the salt produced as a by-product. The solvent was removed by rotary steaming at 50°C. The residue was dissolved in 20 mL of hexane, and the filtering and rotary steaming steps were repeated. Low-boiling-point impurities were removed by distillation under reduced pressure at 60°C. Column chromatography was used to purify the product, which was a pale-yellow transparent liquid, in a high yield of 73.6%. The ^{1}H-NMR and ^{13}C-NMR spectra were obtained using a 400 MHz Instrument (Bruker Corporation, Germany) at 298 K with TMS as the internal standard and CDCl3 as the solvent. IR spectra were recorded on a Nicolet 5700 instrument (Thermo Electron Corporation, Waltham, MA, USA) at room temperature.

The series of methacrylate monomers were numbered a1, b1, c1, d1, and e1, in line with increasing silicon content, and the five acrylate monomers were numbered a2, b2, c2, d2, and e2. The a1 and a2 monomers were purchased and were used as references. All the monomers except a1, a2, were synthesized using the procedure described above. Their chemical structures are shown in Table I; they were all identified by IR, ^{1}H-NMR, and ^{13}C-NMR; the results are as follows:

b1: IR spectrum (KBr): ν = 1720.1 (ν_s; C=O), 1638.1 (ν_s; C=C), 1259.0, 801.0 cm^{-1} (w; Si—CH_3); ^{1}H-NMR (400 MHz, $CDCl_3$, δ): 5.97 (s, 2H, CH=C—C=O), 5.42 (s, 2H, CH=C—C=O), 4.09 (m, 4H, O—CH_2—C), 3.77 (m, 4H, C—CH_2—O), 1.79 (s, 6H, CH=C(CH_3)C=O), −0.0002 (s, 6H, Si—CH3); ^{13}C-NMR (100 MHz, $CDCl_3$, δ): 166.86 (C=O), 135.20, 125.09 (C=C), 65.53, 60.51 (C—O), 17.40 (CH3), −0.0036 (C—Si). Yield: 79.7%.

c1: IR spectrum: ν = 1716.8 (ν_s; C=O), 1638.3 (ν_s; C=C), 1260.3, 801.0 cm^{-1} (w; Si—CH3); ^{1}H-NMR (400 MHz, $CDCl_3$, δ): 6.00 (s, 2H, CH=C—C=O), 5.44 (s, 2H, CH=C—C=O), 4.11 (m, 4H, O—CH_2—C), 3.77 (m, 4H, C—CH_2—O), 1.82 (s, 6H, CH=C(CH_3)C=O), −0.0002 (s, 12H, Si—CH_3); ^{13}C-NMR (100 MHz, $CDCl_3$, δ): 166.27 (C=O), 137.44, 126.80 (C=C),

Table I. Chemical Structures, Names, Silicon Contents, and Yields of Synthetic Monomers and Reagents

Chemical structure	R	n	Sample name	Silicon content (%)	Yield (%)
	CH_3	0	b1	8.86	79.7
	CH_3	1	c1	14.4	74.4
	CH_3	2	d1	18.1	71.6
	CH_3	3	e1	20.8	69.4
	H	0	b2	9.72	77.4
	H	1	c2	15.5	73.6
	H	2	d2	19.3	67.8
	H	3	e2	22.0	63.8
	CH_3		a1	0	
	H		a2	0	

66.84, 61.51 (C—O), 19.46 (CH3), −0.0036 (C—Si). Yield: 74.4%.

d1: IR spectrum: ν = 1720.4 (ν_s; C=O), 1638.5 (ν_s; C=C), 1260.8, 802.7 cm^{-1} (w; Si—CH_3). ^{1}H-NMR (400 MHz, $CDCl_3$, δ): 6.01 (s, 2H, CH=C—C=O), 5.45 (s, 2H, CH=C—C=O), 4.12 (m, 4H, O—CH_2—C), 3.78 (m, 4H, C—CH_2—O), 1.84 (s, 6H, CH=C(CH_3)C=O), −0.0002 (m, 18H, Si—CH_3). ^{13}C-NMR (100 MHz, $CDCl_3$, δ): 168.47 (C=O), 137.37, 126.68 (C=C), 66.79, 61.44 (C—O), 19.41 (CH_3), −0.0035 (C—Si). Yield: 71.6%.

e1: IR spectrum: ν = 1723.9 (ν_s; C=O), 1638.7 (ν_s; C=C), 1261.1, 802.1 cm^{-1} (w; Si—CH_3). ^{1}H-NMR (400 MHz, $CDCl_3$, δ): 6.01 (s, 2H, CH=C—C=O), 5.45 (s, 2H, CH=C—C=O), 4.12 (m, 4H, O—CH_2—C), 3.78 (m, 4H, C—CH_2—O), 1.84 (s, 6H, CH=C(CH_3)C=O), −0.0002 (m, 24H, Si—CH_3). ^{13}C-NMR (100 MHz, $CDCl_3$, δ): 166.64 (C=O), 135.50, 124.86 (C=C), 64.95, 59.50 (C—O), 17.57 (CH_3), −0.0035 (C=Si). Yield: 69.4%.

b2: IR spectrum: ν = 1727.7 (ν_s; C=O), 1636.2, 1620.1 (ν_s; C=C), 1260.1, 801.1 cm^{-1} (w; Si—CH3). ^{1}H-NMR (400 MHz, $CDCl_3$, δ): 6.26 (d, 2H, CH=C), 6.00 (m, 2H, C=CH—C=O), 5.69 (d, 2H, CH=C), 4.09 (m, 4H, C—CH_2—O), 3.76 (m, 4H, O—CH_2—C), −0.0002 (s, 6H, Si—CH_3). ^{13}C-NMR (100 MHz, $CDCl_3$, δ): 165.06 (C=O), 129.87, 127.28 (C=C), 64.46, 59.55 (C—O), −0.0036 (C—Si). Yield: 77.4%.

c2: IR spectrum: ν = 1728.1 (ν_s; C=O), 1636.7, 1620.6 (ν_s; C=C), 1261.3, 804.6 cm^{-1} (w; Si—CH_3). ^{1}H-NMR (400 MHz, $CDCl_3$, δ): 6.30 (dd, 2H, CH=C), 6.04 (m, 2H, C=CH—C=O), 5.75 (dd, 2H, CH=C), 4.13 (m, 4H, C—CH_2—O), 3.78 (m, 4H, O—CH_2—C), −0.0002 (m, 12H, Si—CH_3). ^{13}C-NMR (100 MHz, $CDCl_3$, δ): 167.28 (C=O), 132.06, 129.46 (C=C), 66.68, 61.45 (C—O), −0.0036 (C—Si). Yield: 73.6%.

d2: IR spectrum: ν = 1731.1 (ν_s; C=O), 1636.9, 1620.8 (ν_s; C=C), 1261.8, 803.7 cm^{-1} (w; Si—CH3). ^{1}H-NMR (400 MHz, $CDCl_3$, δ): 6.30 (d, 2H, CH=C), 6.02 (m, 2H, C=CH—C=O), 5.71 (d, 2H, CH=C), 4.12 (m, 4H, C—CH_2—O), 3.78 (m, 4H, O—CH_2—C), −0.0002 (m, 18H, Si—CH_3). ^{13}C-NMR (100 MHz, $CDCl_3$, δ): 167.20 (C=O), 131.90, 129.43 (C=C), 66.62, 61.32 (C—O), −0.0035 (C—Si). Yield: 67.8%.

e2: IR spectrum: ν = 1731.5 (ν_s; C=O), 1636.8, 1620.9 (ν_s; C=C), 1261.2, 803.9 cm^{-1} (w; Si—CH_3). ^{1}H-NMR (400 MHz, $CDCl_3$, δ): 6.31 (d, 2H, CH=C), 6.05 (m, 2H, C=CH—C=O), 5.74 (d, 2H, CH=C), 4.16 (m, 4H, C—CH_2—O), 3.80 (m, 4H, O—CH_2—C), −0.0002 (m, 24H, Si—CH_3). ^{13}C-NMR (100 MHz, $CDCl_3$, δ): 165.19 (C=O), 129.91, 127.40 (C=C), 64.62, 59.28 (C—O), −0.0036 (C—Si). Yield: 63.8%.

Viscosity

Viscosities were measured using a capillary viscometer (Chinese Glass Instrument Factory, Shenyang, China) at 25°C. The following formula was used to calculate viscosity:

$$\nu = ct \times (g_0/g') \quad (1)$$

where ν represents the viscosity, t represents the time the sample takes to flow between two marks, c is a parameter of the capillary viscometer, and g_0 and g' are the standard and local gravitational acceleration, respectively.

Thermogravimetric Analysis

Thermogravimetric analysis (TGA) of the monomers was carried out using a Mettler Toledo TGA/DSC 1/1100 instrument. The weight of the sample used was 5 mg, and specimens were heated from 25 to 600°C at a constant rate of 10°C min^{-1} in air.

Coating and Curing Processes

Ten different polymerization samples were prepared using 10 monomers with 1.5 wt % ITX and 1.5 wt % Irgacure 907. ITX and Irgacure 907 were dissolved in THF with the concentration of 1% in advance. To examine the surface free energy, and for X-ray photoelectron spectroscopy (XPS) measurements, the samples were coated on glass plates, dried with warm air, covered with a plastic wrap, equipped with a nitrogen inlet, and then cured using a low-pressure mercury UV-lamp for 30 min. The light intensity was about 30 μW cm^{-2}, measured at a wave-length of 365 nm. The samples were then dried in an oven at 60°C for 30 min; films of thickness 0.2 mm were obtained. To prepare free standing film samples for the photo-differential scanning calorimetry (DSC) analysis, the samples were cast on an aluminum pan and dried at room temperature for 30 min until the weight no longer changed. The dried films were then irradiated by a UV-light source (200 W miniature arc lamp with 320–500 nm filter and 5 mm crystal optical fiber, EFOS Lite, Canada). The light intensity was determined using a UV-light radiometer (Photoelectric Instrument Factory of Beijing Normal University, Beijing, China). The UV–vis absorption spectra were recorded on a Hitachi U-3010 UV–vis spectrophotometer (Hitachi High-Technologies Corporation, Tokyo, Japan) at 298 K, using acetonitrile as the solvent.

Curing Behavior and Characterization Properties

UV-Curing Behavior by Photo-DSC. The photo-DSC experiments were carried out using a DSC (Q-2000, TA Instruments) instrument equipped with a photocalorimetric accessory. The light intensity was determined by placing an empty DSC pan on the sample cell. The UV light intensity at the sample was 30 mW cm^{-2}. The sample weight was ~5 mg and it was placed in an open aluminum DSC pan to a thickness of 10 μm. The solvent in the sample was removed by evaporation at room temperature for 30 min prior to UV-curing. The measurements were carried out at 25°C in nitrogen gas flowing at 50 mL min^{-1}.

Surface Free Energy. The surface free energies of the UV-cured films were evaluated from the static contact angles, measured using a contact angle analyzer (OCA15-EC, Dataphysics Instruments, Germany). The temperature and relative humidity were 23 ± 1.5°C and 55 ± 5%, respectively. The equilibrium contact angle is defined as the angle between the solid surface and a tangent drawn on the drop-surface, passing through the atmosphere–liquid–solid triple-point.[16]

The surface free energy was calculated from the contact angles, based on Young's equation. In this study, the three liquids method suggested by Good and Van Oss was used. This method has been used widely to examine the surface free energies of polymeric coating films.[17] The three test liquids used were

distilled water, formamide, and diiodomethane. The surface free energy can be calculated from the contact angles of the liquids using the following equations:

$$\gamma_{LV1}(1+\cos\theta_1)=2(\gamma_S^{LW}\gamma_{LV1}^{LW})^{1/2}+(\gamma_S^{+}\gamma_{LV1}^{-})^{1/2}+(\gamma_S^{-}\gamma_{LV1}^{+})^{1/2}$$
$$\gamma_{LV2}(1+\cos\theta_2)=2(\gamma_S^{LW}\gamma_{LV2}^{LW})^{1/2}+(\gamma_S^{+}\gamma_{LV2}^{-})^{1/2}+(\gamma_S^{-}\gamma_{LV2}^{+})^{1/2}$$
$$\gamma_{LV3}(1+\cos\theta_3)=2(\gamma_S^{LW}\gamma_{LV3}^{LW})^{1/2}+(\gamma_S^{+}\gamma_{LV3}^{-})^{1/2}+(\gamma_S^{-}\gamma_{LV3}^{+})^{1/2}$$
$$\gamma=\gamma_S^{LW}+\gamma_S^{AB}=\gamma_S^{LW}+2(\gamma_S^{+}\gamma_S^{-})^{1/2} \quad (2)$$

where LW is the Lifshitz-van der Waals interaction and AB is the acid-base interaction, γ represents the surface free energy including Lifshitz-van der Waals (γ^{LW}) and acid-base interactions (γ^{AB}), and γ^+ and γ^- are the Lewis acid and Lewis base parameters of the surface free energy, respectively; γ_{LV} represents the surface tension of the liquid in equilibrium with its own vapor. The subscripts 1, 2, and 3 denote liquids 1, 2, and 3, respectively. Since γ_{LV}^{LW}, γ_{LV}^{+}, γ_{LV}^{-}, and γ_{LV} are all available (shown in Table S1 in the Supporting Information), the surface free energy can be obtained by solving eq. (2).[18,19]

X-ray Photoelectron Spectroscopy. XPS is a powerful technique for analyzing the surface composition and has been widely used in chemistry, and materials and surface sciences. XPS was performed using an X-ray photoelectron spectrometer (Thermo ESCALAB 250). The excitation source was an Al Kα (1486.6 eV) anode. Constant analyzer energy mode was used at a pass energy of 30.0 eV, and a step of 0.050 eV was used to acquire high resolution spectra of silicon 1s (Si_{1s}), carbon 1s (C_{1s}), and oxygen 1s (O_{1s}). The silicon content at the surface was determined from the peak area, and the ability to transfer to the surface was evaluated by the surface enrichment factor (S_F).

RESULTS AND DISCUSSION

Viscosity

Viscosity is an important property of monomers. The lower the viscosity, the better the leveling properties. The monomers synthesized had low viscosities and were appropriate for use as UV-curing resists. A capillary viscometer can be used to determine the viscosity of a liquid from the flow velocity. (Figure S1 in the Supporting Information, shows the viscosities of the 10 synthetic monomers; Supporting Information Table S2 lists the detailed viscosity data.) According to the experimental data, the monomers with low silicon contents had lower viscosities than the silicon-free monomers. As the silicon content increased, the viscosity of the monomer also increased because materials with higher molar masses usually have higher viscosities.

Thermal Properties Determined by TGA

The thermal properties of monomers play a major role in determining their applications. The thermal properties were determined by TGA at temperatures ranging from 25 to 600°C in air. The results showed that silicon-containing monomers had obvious advantage in terms of thermal stability compared with silicon-free monomers, and could be kept stably below 100°C.

Figure S2(a,b) in the Supporting Information shows the weight loss curves of methacrylate and acrylate monomers, respectively. Table II lists the characteristic thermal decomposition temperatures of the monomers: the temperature of the initial 10% weight loss ($T_{10\%}$), the temperature of 50% weight loss ($T_{50\%}$), and the maximum decomposition temperature (T_{max}). The thermal stabilities of the monomers with two to four silicon atoms were better than those of the monomers with only one silicon atom.

The thermal degradation mechanism of silicon-containing methacrylate monomers had three stages. The first part of the decomposition at 140–188°C, was ester decomposition to methacrylic acid and then liberation of water to give methacrylic anhydride as the ultimate involatile residue. The second decrease, at 228–289°C, was attributed to degradation of the silicon-containing soft segments. The final decomposition, at 392–411°C, was correlated with intermolecular or intramolecular rearrangements, with the formation of silicon-containing cyclic organic products of low molecular weight, which were volatile at high

Table II. Characteristic Thermal Decomposition Data of 10 Monomers

	Weight loss		Maximum decomposition temperature		
Samples	$T_{10\%}$ (°C)[a]	$T_{50\%}$ (°C)[b]	T_{max1}[c]	T_{max2}	T_{max3}
a1	134.2	198.2	170.0		
b1	155.4	231.2	147.2	228.2	410.3
c1	227.9	284.5	140.0	286.2	411.2
d1	232.2	321.0	179.0	284.5	372.1
e1	203.6	292.5	188.8	289.4	399.7
a2	112.0	150.7	161.5		
b2	134.2	198.2	181.9	434.3	
c2	379.4	430.1	124.8	427.2	
d2	367.0	424.6	160.0	422.6	
e2	188.4	427.5	182.0	428.4	

[a] $T_{10\%}$, 10 wt % loss temperature.
[b] $T_{50\%}$, 50% loss temperature.
[c] T_{max}, maximum decomposition temperature.

temperatures.[20] However, the decomposition of methacrylate had only one stage namely the first step above.

For the silicon-containing acrylate monomers, there were only two decomposition stages. The initial stage (125–182°C) was assigned to scission at some unspecified point in the molecule, creating radicals that abstracted hydrogen atoms from the backbone and led to stable radicals.[21] The second stage (416–434°C) was rearrangement and volatilization of the remaining silicon-containing products in a manner similar to that of the methacrylate monomers. The acrylate monomer without silicon only underwent the first stage. The differences between silicon-containing monomers in the same series could be attributed to the stereochemistries of the monomers and different silicon-containing products formed at high temperatures.

UV-Curing Kinetics Determined by Photo-DSC

Photo-DSC is a convenient method of examining UV-curing reactions because it can be used to determine the kinetic parameters, reaction enthalpies, and conversions and curing rates during rapid UV-curing reactions. The UV-curing behavior depends on the intensity of the UV-light, the reaction temperature, the characteristics of the monomers and the photoinitiator, and the reactivities of the functional groups.[22] Photopolymerization has always been a focus of coating research because it gives rapid curing, high-energy efficiency, and low volatile organic contents.[23] The most important parameters characterizing the curing behaviors of an oligomer are the maximum curing rate and the final conversion. The assessment shows that silicon-containing monomers performed better in UV-curing procedures than the silicon-free ones, seen from their much higher final conversions and curing rates.

In this study, photo-DSC was performed to examine the effects of the silicon content on the UV-curing behavior. Figure 1 shows the results of calculations based on the photo-DSC experiments. Photo-DSC is mainly used to monitor photopolymerization and photo-crosslinking of photosensitive materials. The polymerization exothermicity enables DSC measurements to be performed.[24] The extent of reaction or the conversion of double bonds can be determined by integrating the area under the exothermic peak according to the following equation:[25–27]

$$\alpha = \Delta H_t / \Delta H_0^{\mathrm{theor}} \quad (3)$$

where ΔH_t is the reaction heat evolved at time t and $\Delta H_0^{\mathrm{theor}}$ is the theoretical reaction enthalpy for complete conversion. The $\Delta H_0^{\mathrm{theor}}$ values of methacrylate and acrylate are 54.4 kJ mol^{-1} (13.1 kcal mol^{-1}) and 86.2 kJ mol^{-1} (20.6 kcal mol^{-1}),

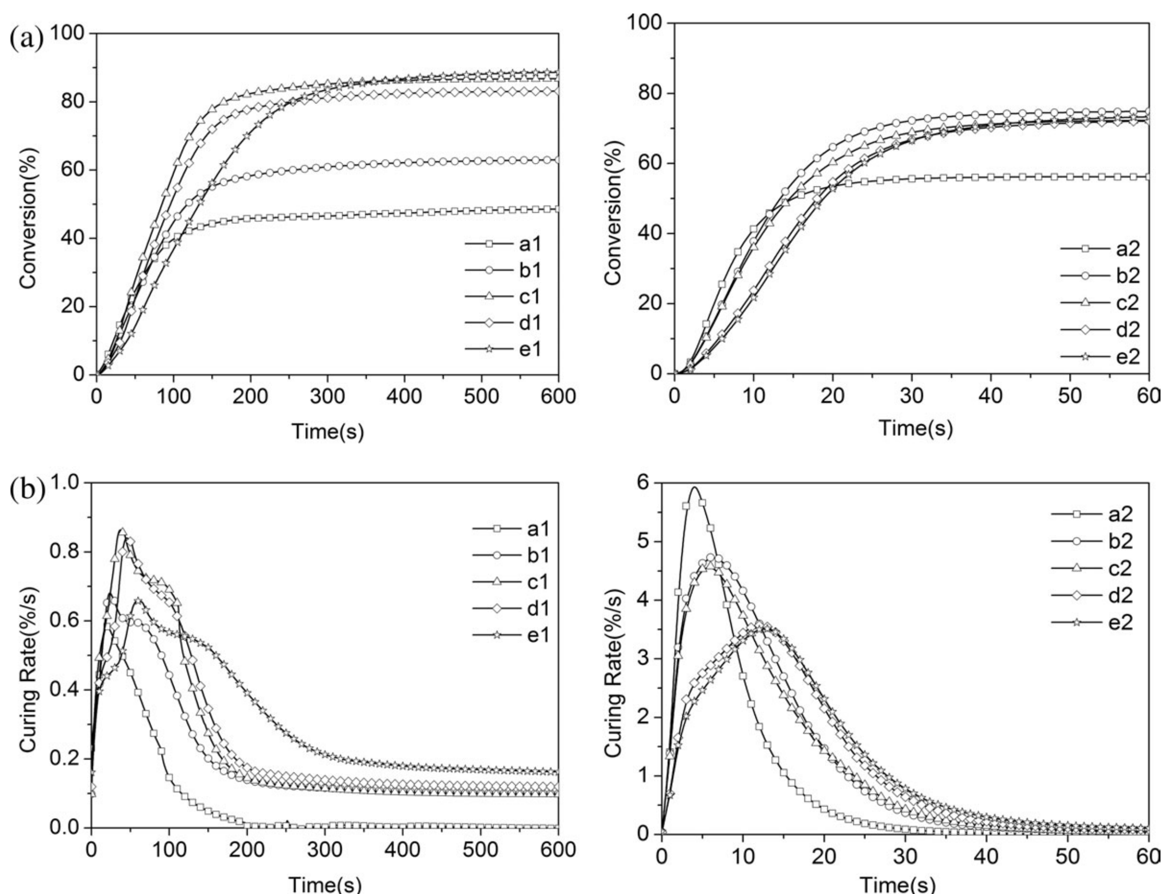

Figure 1. Isothermal UV-curing heat enthalpies and conversion profiles for UV-curable poly(meth)acrylates determined by photo-DSC: (a1) and (a2) conversion vs. time; (b1) and (b2) conversion rate vs. time.

respectively.[22,28] The heat of polymerization of each sample, ΔH_0^{theor} (sample), was calculated using the following equation:

$$\Delta H_0^{theor}\ (\text{sample}) = \Delta H_0^{theor}\ [(\text{meth})\text{acrylate}]/MW^{theor} \times \text{Functionality} \quad (4)$$

where MW^{theor} is the theoretical molecular weight of the repeating unit.[11] (Table S3 in the Supporting Information lists the theoretical reaction enthalpy of each sample.) The rate of polymerization or the curing rate (R_p) is related directly to heat flow (dH/dt) as shown in the following equation:[22,28]

$$R_p = d\alpha/dt = (dH/dt)/\Delta H_0^{theor} \quad (5)$$

where $d\alpha/dt$ is the curing rate, ΔH_0^{theor} represents the total exothermic heat of reaction, and dH/dt is the measured heat flow at a constant temperature.

Figure 1(a1,a2) shows the conversion of each monomer calculated using eqs. (4) and (5). The final conversions were in the following order: e1 > c1 > d1 > b1 > a1 and d2 > e2 > b2 > c2 > a2. Obviously, silicon-containing monomers had higher conversions than silicon-free monomers. The final conversions of the silicon-free methacrylate and acrylate monomers were 48.9 and 56.2%, respectively, whereas those of the e1 and e2 monomers were 89.1 and 76.8%. As Figure 1(b1) shows, the curing rate peak of monomer a1 appeared first at 20 s and the maximum curing rate was 0.584% s^{-1}. The peak time and the maximum curing rate of monomer b1 were 24 s and 0.681% s^{-1}, respectively, which represented a fast photopolymerization reaction. A similar trend was found for the acrylate monomers. Although the silicon content decreased the curing rate to some degree, the higher final conversion would compensate for this disadvantage. Table III shows the peak times of curing rate, maximum curing rate, and final conversion, which further confirm our suggestions.

The curves show that the double-bond conversions of methacrylate monomers were higher than those of acrylate monomers, and the polymerization rates of the former were much slower than those of the latter. Among the silicon-containing monomers, methacrylate monomers with two to four silicon atoms had higher conversions than the other synthetic monomers, but acrylate monomers with one to two silicon atoms had faster curing rates.

Table III. Peak Times of Curing Rates, Maximum Curing Ratse, Peak Conversion, and Final Conversions of UV-Curable Poly(meth)acrylates Determined by Photo-DSC

Samples	Peak time of curing rate (s)	Maximum curing rate (% s^{-1})	Final conversion (%)
a1	20	0.584	48.9
b1	24	0.681	63.3
c1	37	0.864	86.8
d1	45	0.840	83.2
e1	59	0.658	89.1
a2	4	6.08	56.2
b2	6	4.73	75.0
c2	6	4.57	72.8
d2	12	3.57	77.2
e2	13	3.51	76.8

Surface Free Energy

The surface free energy measurements confirmed that the addition of silicon atoms to the soft segment could effectively lower the surface free energy, which further increases the water repellency, antifouling properties, and releasability of the UV-curing resists.

The contact angle and surface free energies of the UV-cured films are shown in Table IV and Figure 2. The contact angle of the UV-cured film increased with increasing silicon content, as silicon decreased the surface free energy. The silicon-containing

Table IV. Contact Angles and Surface Free Energies of UV-Curable Poly(meth)acrylate Films

Samples	Contact angle (°)			Surface free energy (mN m^{-1})[a]		
	Water	Formamid	Diiodomethane	γ_S	γ_S^{LW}	γ_S^{AB}
a1	73.1 ± 0.1	58.8 ± 0.1	50.5 ± 1.0	43.6	34.2	9.4
b1	92.4 ± 1.1	74.4 ± 2.2	61.2 ± 2.0	30.3	27.9	2.4
c1	101.6 ± 2.5	82.7 ± 2.1	70.5 ± 0.8	24.5	22.6	1.9
d1	102.1 ± 0.8	83.2 ± 0.5	71.2 ± 0.2	24.1	22.2	1.9
e1	104.5 ± 0.1	85.4 ± 1.5	77.6 ± 0.7	22.2	18.8	3.4
a2	76.2 ± 0.4	63.4 ± 0.8	57.2 ± 0.4	40.4	30.4	10.0
b2	92.5 ± 0.1	72.4 ± 2.5	61.6 ± 0.6	29.7	27.7	2.0
c2	101.8 ± 0.1	82.1 ± 1.7	72.5 ± 1.2	24.7	21.5	3.2
d2	101.9 ± 0.1	82.7 ± 1.7	72.2 ± 1.7	23.1	21.7	1.4
e2	104.4 ± 0.1	85.0 ± 1.2	74.4 ± 0.1	22.7	20.5	2.2
glass	24.4 ± 0.1	32.6 ± 1.8	41.4 ± 0.1	68.9	38.9	30.0

[a] γ_S = surface free energy; γ_S^{LW} = Lifshitz-van der Waals (dispersive component); γ_S^{AB} = acid-basic interaction (polar component).

monomers showed a sharp decline in surface free energy compared with the monomers without silicon. The surface free energies of a1 and a2 were 48.9 and 50.6 mN m^{-1}, respectively. With the introduction of only one silicon atom, the surface free energies decreased significantly to 30.3 and 29.7 mN m^{-1}. A small amount of silicon significantly affected the surface free energies.

Among the silicon-containing monomers, the surface free energies of monomers with two silicon atoms were much lower than those of monomers with only one silicon atom, but similar to those of monomers with three silicon atoms. The surface free energies of monomers with four silicon atoms were lower. These results suggest that the silicon atoms in the soft segment were transferred to the outermost surface and produced UV-cured films with a hydrophobic silicon enriched surface.

XPS Analysis

In the contact angle measurements, it was found that the water and oil contact angles at the UV cured film surface increased with increasing silicon content, which indicated aggregation of low surface energy components at the interface.[29] However, contact angle analysis cannot give direct and clear information on the types and relative concentrations of different atoms at the surface, and therefore XPS analysis was employed to evaluate the surface characteristics of the hybrid materials independently. XPS was used to investigate the content of various elements at the outermost layer (2–3 nm) of the coatings in a high vacuum.[30] The results agreed well with the variations in surface free energies. The higher the silicon contents at the surface, the lower the surface free energy.

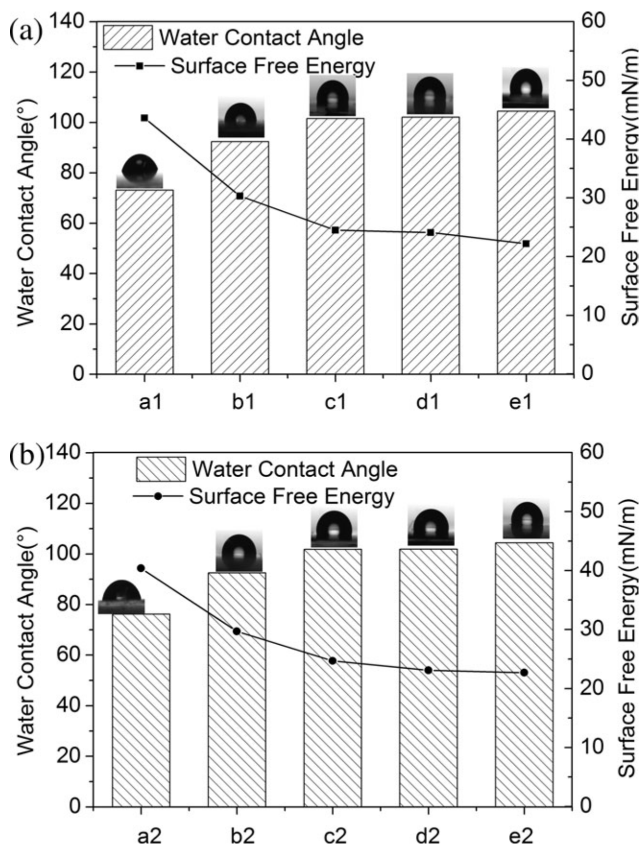

Figure 2. Water contact angles and surface free energies of the UV-cured films: (a) silicon-containing and silicon-free polymethacrylates; (b) silicon-containing and silicon-free polyacrylates.

Figure 3 shows the XPS spectra of the UV-cured films of silicon-containing monomers. The photoemission peaks of the Si_{2p}, O_{1s}, and C_{1s} core levels can be observed with binding energies of 106, 292, and 539 eV, respectively. The surface enrichment factor (S_F) is defined as the ratio of the silicon content measured experimentally at the top surface of the cured film ($F_{surface}$) to the calculated silicon content in the UV-cured film (F_{bulk}):[31]

$$S_F = F_{surface}/F_{bulk} \quad (6)$$

Table V lists the silicon contents in, and at the surfaces of, the UV-cured films and the surface enrichment factors. According to the monomer chemical structures, the silicon atoms would be wrapped up by methyl groups in the inner parts of the molecules because of chemical bonding and steric hindrance.

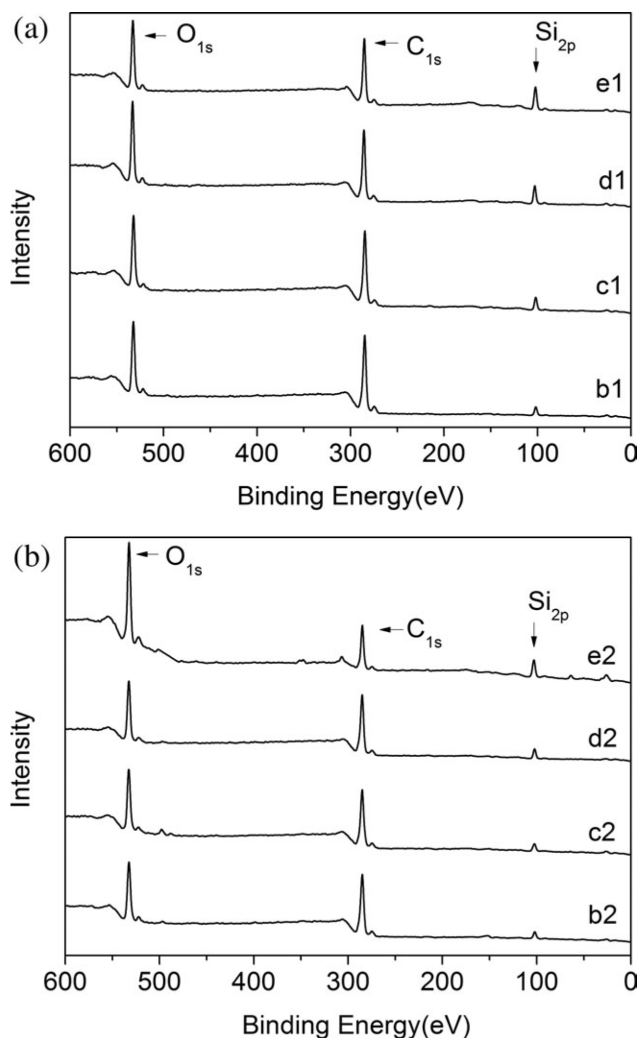

Figure 3. X-ray photoelectron spectra of UV-cured films: (a) silicon-containing polymethacrylates, (b) silicon-containing polyacrylates.

Table V. Silicon Contents at Surfaces of UV-Cured Films and Surface Enrichment Factors

Samples	Si content (wt %) in the UV-cured film (F_{bulk})	Si content (wt %) at the surface ($F_{surface}$)	Surface enrichment (S_F)
b1	8.59	8.01	0.932
c1	13.93	15.60	1.120
d1	17.56	18.79	1.070
e1	20.20	21.16	1.048
b2	9.43	7.562	0.802
c2	15.00	14.00	0.933
d2	18.69	17.10	0.915
e2	21.30	22.26	1.045

The silicon content at the surface of the UV-cured film should therefore be lower than the silicon composition of the polymer. However, similar, or even higher, silicon contents at the surface were obtained experimentally. For example, the F_{bulk} and $F_{surface}$ of monomer c1 were 13.93 and 15.6%, respectively. Thus, the S_F value was calculated as 1.120. This is because the silicon atoms would migrate to the surface, resisting hindrance. As shown in Table V, the silicon content at the film surfaces increased in order, which kept excellent agreement with the surface free energy.

CONCLUSIONS

Eight different silicon-containing (meth)acrylate monomers were synthesized by substitution reactions. Their chemical structures were identified by IR, ^{1}H-NMR, and ^{13}C-NMR spectroscopies. The addition of silicon-containing structures resulted in monomers with excellent UV-curing behaviors, as seen from their higher final conversions and fast curing rates. Moreover, the silicon-containing monomers had better thermal stabilities and significantly lower surface free energies, which can increase their releasabilities and antifouling properties.

Taking economic factors into account, better performances in terms of low surface free energies and UV-curing behaviors at a reasonable cost were found in monomers b1 and b2. These two monomers would therefore be preferable for use in manufacturing.

In conclusion, silicon-containing (meth)acrylate monomers are appropriate for use as photosensitive compounds. Appropriate monomers, mixed with resins and additives according to specific proportions, could be used as antifouling and antifingerprint materials, and in nanoimprinting, microelectronics, and biological materials. Antifouling and antifingerprint materials are the focus of much research, and have a wide range of practical applications such as in decorative coatings and mobile phone screen.

ACKNOWLEDGMENTS

The financial support of the Beijing Natural Science Foundation (2112020) is gratefully acknowledged.

REFERENCES

1. Xie, C.; Shi, W. F. *Prog. Org. Coat.* **2010**, *69*, 252.
2. Decker, C.; Viet, T. N. T.; Decker, D.; Weber-Koehl, E. *Polymer* **2001**, *42*, 5531.
3. Chattopadhyay, D. K.; Panda, S. S.; Raju, K. V. S. N. *Prog. Org. Coat.* **2005**, *54*, 10.
4. Huang, Z. G.; Shi, W. F. *Prog. Org. Coat.* **2007**, *59*, 312.
5. Xiao, X. Y.; Hao, C. C. *Colloids Surf. A.* **2010**, *359*, 82.
6. Valette, L.; Massardier, V.; Pascault, J. P.; Magny, B. *J. Appl. Polym. Sci.* **2002**, *86*, 753.
7. Liu, H. B.; Chen, M. C.; Huang, Z. T.; Xu, K.; Zhang, X. J. *Eur. Polym. J.* **2004**, *40*, 609.
8. Tang, C. Y.; Liu, W. Q.; Ma, S. Q.; Wang, Z. F.; Hu, C. H. *Prog. Org. Coat.* **2010**, *69*, 359.
9. Wu, C. C.; Hsu, S. L. C.; Liao, W. C. *Microelectron. Eng.* **2009**, *8*, 325.
10. Toralla, K. P.; Girolamo, J. D.; Truffier-Boutry, D.; Gourgon, C.; Zelsmann, M. *Microelectron. Eng.* **2009**, *86*, 779.
11. Hwang, H. D.; Kim, H. J. *React. Funct. Polym.* **2011**, *71*, 655.
12. Crivello, J. V.; Lee, J. L. *J. Appl. Polym. Sci.* **1990**, *28*, 479.
13. Sangermano, M.; Bongiovanni, R.; Malucelli, G.; Priola, A.; Olbrych, J.; Harden, A.; Rehnberg, N. *J. Polym. Sci. Part A: Polym. Chem.* **2004**, *42*, 1415.
14. Batten, R. J.; Davidson, R. S.; Ellis, R. J.; Wilkinson, S. A. *Polymer* **1992**, *33*, 3037.
15. Davidson, R. S.; Ellis, R.; Tudor, S.; Wilkinson, S. A. *Polymer* **1992**, *33*, 3031.
16. Gindl, M.; Sinn, G.; Gindl, W.; Reiterer, A.; Tschegg, S. *Colloids Surf. A.* **2001**, *181*, 279.
17. Van Oss, C. J.; Good, R. J.; Chaudhury, M. K. *Langmuir* **1988**, *4*, 884.
18. Lee, Y.K.; Kim, H.J.; Rafailovich, M.; Sokolov, J. *Int. J. Adhes. Adhes.* **2002**, *22*, 375.
19. Geerken, M. J.; Lammertink, R. G. H.; Wessling, M. *Colloids Surf. A.* **2007**, *292*, 224.
20. Grant, D. H.; Grassie, N. *Polymer* **1960**, *1*, 445.
21. Ors, J. A.; La Perriere, D. M. *Polymer* **1986**, *27*, 1999.
22. Palanisamy, A.; Rao, B. S. *Prog. Org. Coat.* **2007**, *60*, 161.
23. Asif, A.; Shi, W. F.; Shen, X. F.; Nie, K. M. *Polymer* **2005**, *46*, 11066.
24. Rao, B. S.; Palanisamy, A. *Prog. Org. Coat.* **2010**, *67*, 6.
25. Qazvini, N. T.; Mohammadi, N. *Polymer* **2005**, *46*, 9088.
26. Dietz, J. E.; Peppas, N. A. *Polymer* **1997**, *38*, 3767.
27. Sirotkin, R. O.; Brooks, N. W. *Polymer* **2001**, *42*, 9801.
28. Yu, Q.; Nauman, S.; Santerre, J. P.; Zhu, S. *J. Appl. Polym. Sci.* **2001**, *82*, 1107.
29. Miao, H.; Cheng, L. L.; Shi, W. F. *Prog. Org. Coat.* **2009**, *65*, 71.
30. Fabbri, P.; Messori, M.; Montecchi, M.; Nannarone, S.; Pasquali, L.; Pilati, F.; Tonelli, C.; Toselli, M. *Polymer* **2006**, *47*, 1055.
31. Hwang, H. D.; Kim, H. J. *J. Colloid Interface Sci.* **2011**, *362*, 274.